JOURNAL OF GUIDANCE, CONTROL, AND DYNAMICS
Vol. 24, No. 3, May–June 2001

Mixed Norm Control of a Helicopter

Michael Trentini and Jeff K. Pieper
University of Calgary, Calgary, Alberta T2N 1N4, Canada

Presented is the design and analysis of robust full authority flight controllers to improve the handling qualities of a fly-by-wire Bell 205 helicopter. The emphasis is to meet stringent U.S. Army handling qualities specifications against the constraint of robust stability. The designer goal is to reproduce specifications constituting an ideal target model in the actual Bell 205, which does not naturally exhibit good handling qualities. A solution to robust flight controllers is a mixed-norm control design methodology that incorporates both optimal nominal model-following performance and robust stability objectives. Mixed-norm optimization addresses an outstanding problem in helicopter flight control, which has been the unrealistic mapping of multiple design objectives into a single norm. Error dynamics between the response of the model and the actual helicopter are explicitly defined from experimental data to reduce the performance vs robustness tradeoff. The mixed-norm control problem addresses genuine system requirements without compromise. Analysis and simulation results show an effective robust controller designed for the Bell 205.

Nomenclature

A_0, B_0, C_0, D_0	=	state transition, control input mapping, and output mappings
H_2, H_∞	=	Hardy spaces
$H_{2/\infty}, J_{2/\infty}$	=	mixed-norm problem Hamiltonians
K	=	dynamic controller
$U, W, Q, V, P, R, \theta, \phi$	=	state components (forward and lateral velocity, pitch rate, vertical velocity, roll and yaw rates, and pitch and roll attitudes)
$\boldsymbol{u}, \boldsymbol{\theta}$	=	control and control derivative vectors
$X_{2/\infty}, Y_{2/\infty}$	=	mixed-norm problem Riccati solutions
$\boldsymbol{x}_0, \boldsymbol{\xi}_0$	=	state vectors
$\boldsymbol{\delta}_0$	=	control surfaces
τ_0, ξ, ω_n	=	time constant, damping ratio, and natural frequency of error description

I. Introduction

THE manual piloting of helicopters is challenging and mentally taxing due to their inherent instabilities and highly nonlinear, cross-coupled nature. It is difficult to design and build helicopters that naturally exhibit good handling qualities. For example, at low speed without mechanical feedback, the single-rotor helicopter is naturally unstable. The coupled pitch/roll pendulum instability is a product of the flapping rotors' response to velocity perturbations. Corrective control inputs that are necessary to maintain hover require considerable attention of the pilot and limit the desired flight path. Furthermore, if visual cues degrade, so that the pilot has difficulty perceiving attitude and velocity, then the hover task becomes increasingly difficult.[1] These shortcomings motivate the design of flight control systems to provide acceptable handling qualities and reduce pilot workload.

Whereas the design of flight control systems (FCS) for fixed-wing aircraft is a mature discipline,[2] application of control theory to helicopters is much less well developed and is more complex.[3] The control of a helicopter is a genuinely multivariable problem in which one usually considers four inputs and four outputs with significant interaxis coupling. True multivariable analysis and design for helicopter flight control can potentially provide improved performance in the on-axis loops while offering good decoupling behavior.[4,5] Moreover, the use of modern multivariable control analysis tools allows a more rigorous analysis and, consequently, improved stability robustness of the closed-loop system.[6] Multivariable design of rotorcraft flight control systems for performance and robustness has been studied recently, including eigenstructure assignment,[7–10] sliding mode control,[11] H_2 design,[3,12] and H_∞ optimization.[13] The outstanding problem has been the inability to map realistic design objectives into a single norm, which the synthesis methods then optimize. Although the H_2 and H_∞ norms may often be genuine design objectives, to combine all of the objectives using a single norm as a cost function requires compromise. For example, linear quadratic synthesis results in a controller adept at providing optimal nominal performance but with potentially weak robustness characteristics, even though it often works well within its known 60-deg phase margin. Similarly, an H_∞ controller results in a highly robust system with potentially poor performance. Recently, there has been a great deal of interest in formulating a mixed H_2/H_∞ control methodology,[14] where the H_2 performance subject to an upper bound on the H_∞ norm is optimized.[15] The H_∞-norm bound delivers a certain stability margin and the H_2 norm represents a (scalar) performance measure, related to the energy content of the output. Early approaches included solving the problem for one and two block problems.[16–21] A mixed H_2/H_∞-norm problem with two exogenous input vectors and two controlled output vectors has been developed for full state feedback.[22]

This paper documents research extending from work directed at the design of flight controllers on a Bell 205 helicopter.[3] It presents a critical assessment of the use of mixed H_2/H_∞ control in the design

Michael Trentini received a B.Sc. from Queen's University in 1993 and a Ph.D. from the University of Calgary in 1999, both in mechanical engineering. He is currently employed by Revolve Technologies, working on control of magnetic bearings. His research interests include flight control and robust control.

Jeff Pieper graduated from Queen's University in 1987 with a B.Sc. in mechanical engineering and then from the University of California at Berkeley in 1988 with an M.S. in mechanical engineering. In 1992 he received a Ph.D. in mechanical engineering from Queen's University. He has held research positions at Alcan Aluminum, Carleton University, and the National Research Council of Canada Institute for Aerospace Studies. He is currently an Associate Professor and Director of the Mechanical Engineering Program at the University of Calgary.

Received 17 September 1999; revision received 12 July 2000; accepted for publication 13 July 2000.

of robust flight controllers for the Bell 205 operating in a steady hover condition. The emphasis in the design is to meet stringent U.S. Army handling qualities specifications against the constraint of robust stability to plant perturbations. The problem is formulated as a robust stability problem with optimal nominal performance. The optimal nominal performance is cast as a model-following design optimization of a target model from military handling qualities specifications. Robustness to plant uncertainty is based on experimental and analytical models that result in a linear fractional transformational description of the uncertain system. Structured singular value analysis is used to identify stable limits on variation in aircraft dynamics.

II. Aircraft Modeling

The aircraft considered is a Bell 205 helicopter, fully instrumented with all relevant aircraft states measurable and full authority fly-by-wire actuation.[23] The Bell 205 is a single-turbine aircraft with a two-bladed teetering main rotor and an antitorque tail rotor.

A. Low-Order Helicopter Model

Six-degree-of-freedom linear models of the Bell 205 are available at a variety of trim points.[24] The steady hover condition is used as the trimmed operating condition because this is the starting point for important helicopter tasks such as precision hovering. The low-order model in Eq. (1) for the Bell 205 (Ref. 24) represents the aircraft trimmed at a nominal +5-deg pitch attitude, midrange weight, midposition center of gravity, and operating in-ground effect at near sea level and in nominal steady hover condition. The model is described by

$$\dot{\boldsymbol{x}}_h = A_h \boldsymbol{x}_h + B_h \boldsymbol{u} \tag{1}$$

$$A_h = \begin{bmatrix} 0 & 0.03 & 0.18 & -0.01 & -0.42 & -0.08 & -9.81 & 0 \\ -0.10 & -0.39 & 0.09 & -0.10 & -0.12 & 0.68 & 0 & 0 \\ 0.01 & -0.01 & -0.19 & 0 & 0.23 & 0.04 & 0 & 0 \\ 0.02 & 0 & -0.41 & -0.05 & -0.27 & 0.27 & 0 & 9.81 \\ 0.03 & -0.02 & -0.88 & -0.04 & -0.57 & 0.14 & 0 & 0 \\ -0.01 & -0.02 & -0.06 & 0.07 & -0.32 & -0.71 & 0 & 0 \\ 0 & 0 & 1 & 0 & 0 & 0 & 0 & 0 \\ 0 & 0 & 0 & 0 & 1 & 0 & 0 & 0 \end{bmatrix}$$

$$B_h = \begin{bmatrix} 0.08 & 0.13 & 0 & 0 \\ -1.17 & 0.04 & 0 & 0.01 \\ 0 & -0.07 & 0 & 0.01 \\ -0.04 & 0 & 0.11 & 0.20 \\ -0.04 & 0 & 0.22 & 0.17 \\ 0.17 & 0 & 0.03 & -0.47 \\ 0 & 0 & 0 & 0 \\ 0 & 0 & 0 & 0 \end{bmatrix}$$

$$\boldsymbol{x}_h = \begin{bmatrix} U \\ W \\ Q \\ V \\ P \\ R \\ \theta \\ \phi \end{bmatrix} = \begin{bmatrix} \text{forward velocity} \\ \text{vertical velocity} \\ \text{pitch rate} \\ \text{lateral velocity} \\ \text{roll rate} \\ \text{yaw rate} \\ \text{pitch attitude} \\ \text{roll attitude} \end{bmatrix}$$

$$\boldsymbol{u} = \begin{bmatrix} \delta_C \\ \delta_B \\ \delta_A \\ \delta_P \end{bmatrix} = \begin{bmatrix} \text{collective} \\ \text{longitudinal cyclic} \\ \text{lateral cyclic} \\ \text{tail rotor collective} \end{bmatrix}$$

Angular rates are in units of radians per second, translational rates in meters per second, and attitudes in radians. Control inputs are in terms of pilot stick movement in centimeters.

B. Uncertainty Description

The teetering rotor implies that body rotational and translational motion are a result of a high-order process involving the cockpit stick, actuators, rotor tip path plane, and, finally, body motion. Low-order aircraft models do not fully describe these characteristics, and so it is necessary to study the associated uncertainty dynamics. The uncertain error dynamics in the low-order nominal model (1) result from a variety of sources including 1) unmodeled rotor modes, 2) unmodeled high-frequency body and rotor mast flexing modes, 3) unmodeled sensor and actuator dynamics, and 4) other discrepancies due to high-order effects.

To assess the model fidelity and quantify the error dynamics associated with the true aircraft, frequency-domain comparisons between the nominal model and the aircraft were conducted. The experimental aircraft response was found through fast Fourier transform (FFT) graphs evaluated across the frequency spectrum of interest from flight time histories. Experience with this type of testing has shown that a manual pilot-induced frequency sweep of each input gives sufficient frequency information to allow confidence in the results. The pilot minimized off-axis inputs so that cross-coupling stability and control derivatives could be more accurately analyzed.

A typical experimental result of frequency sweep testing is shown in Fig. 1, indicating magnitude and phase for longitudinal cyclic input to pitch rate output. The coherence function, a measure of variance normalized and subtracted from one, indicates the reliability of the experimental data found by taking several overlapping windows (10 each of length 64 s) on the time histories and computing the FFT. The lack of strong coherence at low (0.1–0.4 rad/s) and very high frequencies (13–20 rad/s) is a function of the manually piloted input frequency sweeps that do not fully cover the spectrum of interest. The solid line in Fig. 1 shows the predicted system response based on the linear model of Eq. (1).

Comparison of the model response to the actual aircraft response reveals a modeling error. The model does not include sensor and actuator dynamics. These dynamics are typically first order and fairly fast and affect all channels or axes equally, with the exception of sensor dynamics in pitch and roll attitudes where measurement comes from integration of the respective rates. State-space realizations for the multi-input/multi-output systems representing sensor (subscript s) and actuator (subscript a) dynamics are

$$\dot{\boldsymbol{x}}_s = -1/\tau_s \cdot I_6 \boldsymbol{x}_s + I_6 \boldsymbol{u}_s = A_s \boldsymbol{x}_s + B_s \boldsymbol{u}_s$$

$$y_s = 1/\tau_s \cdot I_6 \boldsymbol{x}_s + 0_{6\times 6} \boldsymbol{u}_s = C_s \boldsymbol{x}_s + D_s \boldsymbol{u}_s \tag{2}$$

$$\dot{\boldsymbol{x}}_a = -1/\tau_a \cdot I_4 \boldsymbol{x}_a + I_4 \boldsymbol{u}_a = A_a \boldsymbol{x}_a + B_a \boldsymbol{u}_a$$

$$y_a = 1/\tau_a \cdot I_4 \boldsymbol{x}_a + 0_{4\times 4} \boldsymbol{u}_a = C_a \boldsymbol{x}_a + D_a \boldsymbol{u}_a \tag{3}$$

where $\tau_s = 0.06$ s and $\tau_a = 0.03$ s.

Of primary importance in achieving high-bandwidth control of the Bell 205 is the rotor mast-flexing mode, which involves movement of the transmission and rotor mast constrained by the engine mounts and other linkages. It appears in the experimental frequency-response plots as a resonant peak at about 14 rad/s, and the damping ratio is estimated at 0.15. The rotor mast-flexing mode occurs when collective, longitudinal, or lateral cyclic controls are applied. The mode is relatively fast and, thus, appears in the rate modes of the aircraft associated with their most influential input. It is assumed that this mode will affect the following strong input–output channels equally: 1) collective and vertical velocity, 2) longitudinal cyclic and pitch rate, and 3) lateral cyclic and roll rate. This mode is included more conservatively in the following strongly coupled channels: 4) longitudinal cyclic and roll rate and 5) lateral cyclic and pitch rate. The state-space realization representing rotor mast-flexing mode dynamics (subscript f) is

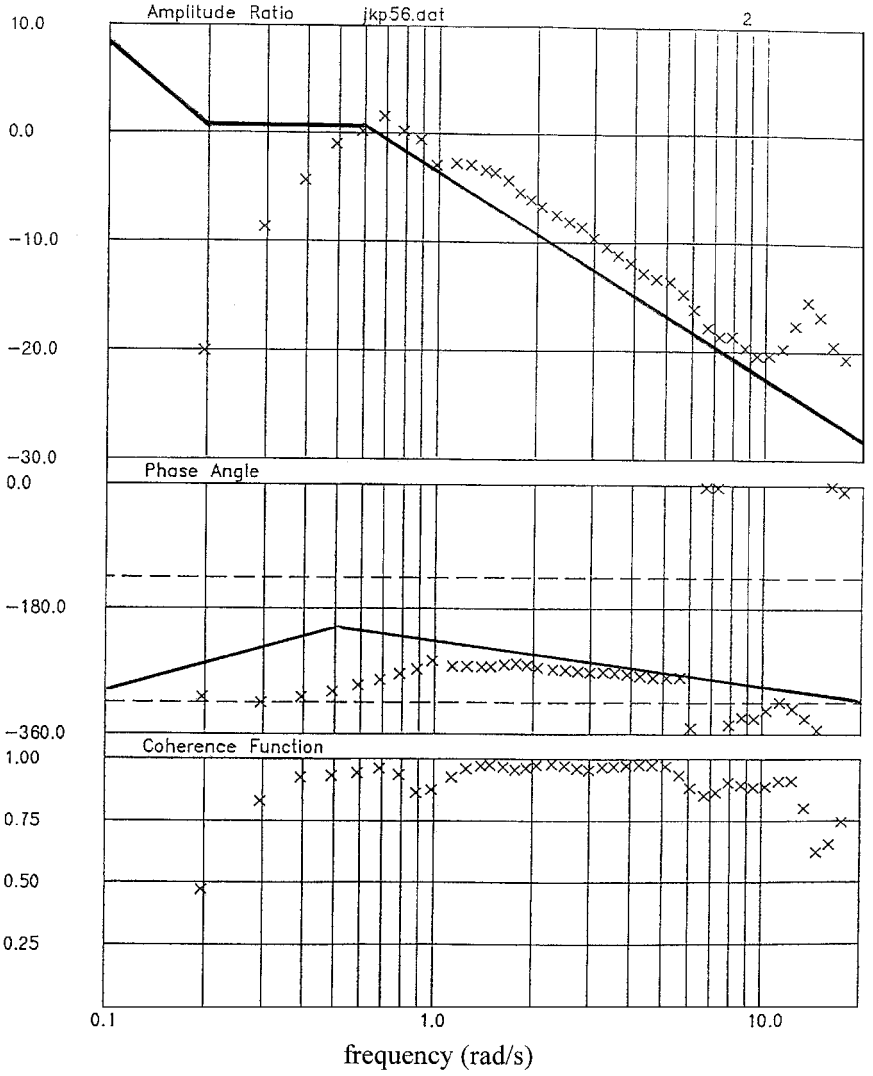

Fig. 1 Experimental frequency response in hover, longitudinal cyclic to pitch rate.

$$\dot{\boldsymbol{x}}_f = \begin{bmatrix} -2\zeta\omega_n & -\omega_n^2 & 0 & 0 & 0 & 0 \\ 1 & 0 & 0 & 0 & 0 & 0 \\ 0 & 0 & -2\zeta\omega_n & -\omega_n^2 & 0 & 0 \\ 0 & 0 & 1 & 0 & 0 & 0 \\ 0 & 0 & 0 & 0 & -2\zeta\omega_n & -\omega_n^2 \\ 0 & 0 & 0 & 0 & 1 & 0 \end{bmatrix} \boldsymbol{x}_f + \begin{bmatrix} 1 & 0 & 0 \\ 0 & 0 & 0 \\ 0 & 1 & 0 \\ 0 & 0 & 0 \\ 0 & 0 & 1 \\ 0 & 0 & 0 \end{bmatrix} \boldsymbol{u}_f = A_f \boldsymbol{x}_f + B_f \boldsymbol{u}_f$$

$$y_f = \begin{bmatrix} 0 & \omega_n^2 & 0 & 0 & 0 & 0 \\ 0 & 0 & 0 & \omega_n^2 & 0 & 0 \\ 0 & 0 & 0 & 0 & 0 & \omega_n^2 \end{bmatrix} \boldsymbol{x}_f + 0_{3\times 3}\boldsymbol{u}_f = C_f \boldsymbol{x}_f + D_f \boldsymbol{u}_f \tag{4}$$

where $\omega_n = 14.0$ rad/s and $\zeta = 0.15$.

An important consideration in modeling the uncertainty is the inclusion of high-frequency unmodeled dynamics, including rotor modes, structural modes, and mechanical component responses that are manifested in the frequency-response curves as additional high-frequency phase lag. The dynamics are modeled as pure delay with a first-order Padé approximation and a conservative estimate of delay, $\tau_d = 100$ ms. This mode is the fastest and is seen mainly in the rotational rates, which are the first aircraft modes to respond to inputs. It is assumed that this mode will affect the following strong input–output channels equally: 1) longitudinal cyclic and pitch rate, 2) lateral cyclic and roll rate, and 3) tail rotor collective and yaw rate, and again more conservatively in the following strongly coupled channels: 4) longitudinal cyclic and roll rate and 5) lateral cyclic and pitch rate.

The state-space realization representing delay (subscript d) is

$$\dot{\boldsymbol{x}}_d = -2/\tau_d \cdot I_3 \boldsymbol{x}_d + I_3 \boldsymbol{u}_d = A_d \boldsymbol{x}_d + B_d \boldsymbol{u}_d$$

$$y_d = 4/\tau_d \cdot I_3 \boldsymbol{x}_d - I_3 \boldsymbol{u}_s = C_d \boldsymbol{x}_d + D_d \boldsymbol{u}_d \tag{5}$$

Finally, low-frequency system/model mismatch is corrected by the inclusion of a lead-lag filter. Typically, it is observed that the model break frequency is lower than that of the actual plant, where the model break frequency is about 1 rad/s, whereas the actual system breaks at 2 rad/s. On investigation of the data, it is necessary to include the low-frequency dynamics in the following input–output channels: 1) collective and vertical velocity, 2) longitudinal cyclic and pitch rate, and 3) lateral cyclic and roll rate, and, more conservatively, in 4) longitudinal cyclic and roll rate and 5) lateral cyclic and pitch rate with the resulting state-space realization for low-frequency errors (subscript l)

$$\dot{\boldsymbol{x}}_l = -1/\tau_t \cdot I_4 \boldsymbol{x}_l + I_4 \boldsymbol{u}_l = A_l \boldsymbol{x}_l + B_l \boldsymbol{u}_l$$

$$y_l = (\tau_t - \tau_m)/\tau_t^2 \cdot I_4 \boldsymbol{x}_l - I_4 \boldsymbol{u}_l = C_l \boldsymbol{x}_l + D_l \boldsymbol{u}_l \tag{6}$$

where $\tau_m = 1.0$ and $\tau_t = 2.0$.

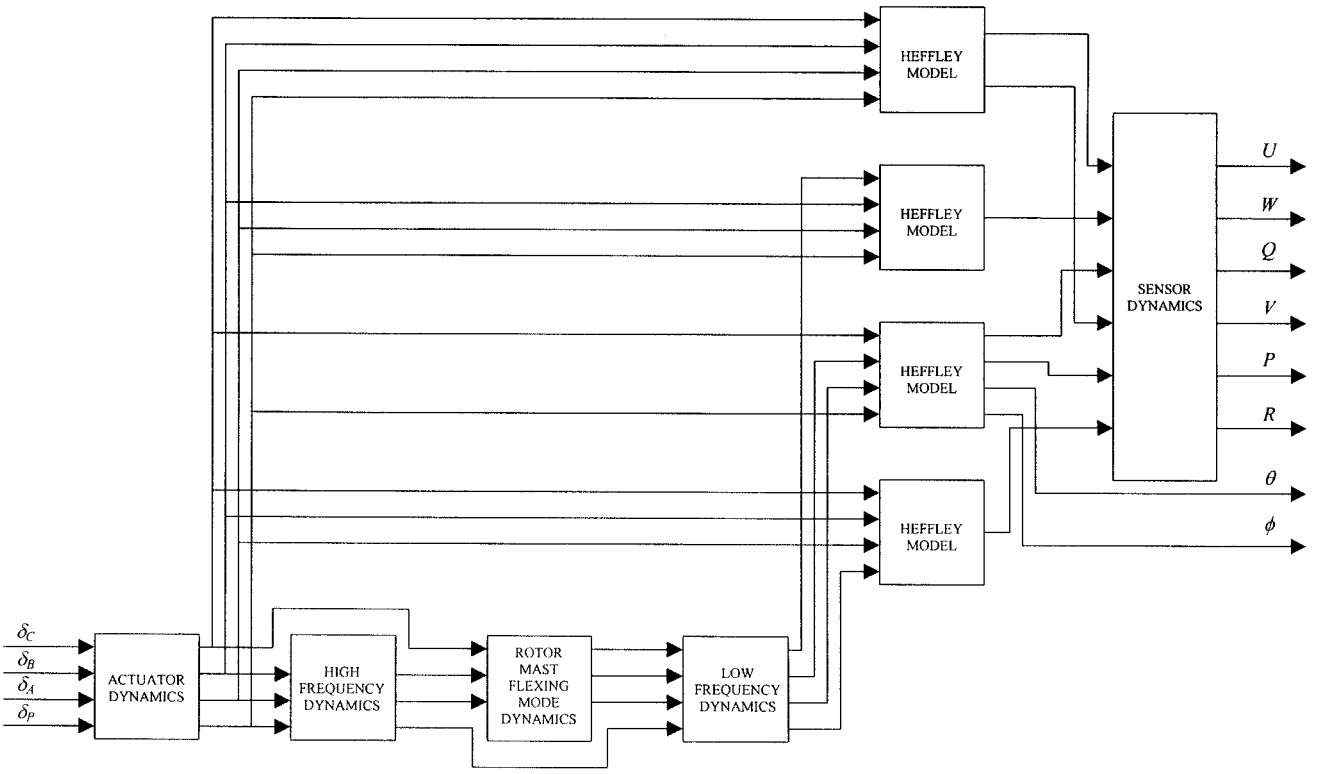

Fig. 2 Interconnection structure of the higher-order model.

C. Higher-Order Helicopter Model

Piecing together the error dynamics of the low-order nominal model with the model itself results in a higher-order model whose frequency-domain response more closely matches the experimental frequency-domain aircraft response. A diagram of the interconnection structure for the higher-order model is depicted in Fig. 2. The blocks in the diagram represent dynamic system components with block diagonal structures described by Eqs. (2–6). They are interconnected with four copies of the nominal model in Eq. (1) to account for all reasonable dynamics of the helicopter. This 67th-order model better represents the Bell 205 helicopter and is described by

$$\dot{\boldsymbol{x}}_{h/e} = A_{h/e}\boldsymbol{x}_{h/e} + B_{h/e}\boldsymbol{u} \tag{7}$$

where the pair $(A_{h/e}, B_{h/e})$ is defined with consistent units.

D. Model Uncertainty

It is unreasonable to assume that dynamic uncertainty can be completely removed from any nominal model of a helicopter. Parametric uncertainty exists in the sensor and actuator dynamics from imperfect knowledge of physical parameter values τ_s and τ_a used to model these subsystems, as well as their variations during operation. The uncertainty used in these parameters is $\pm\frac{1}{10}$ of their nominal values, such that each of the uncertain physical parameter values τ_s and τ_a are bounded, respectively, in the region

$$\left[\tau_s - \tfrac{1}{10}\tau_s,\ \tau_s + \tfrac{1}{10}\tau_s\right], \qquad \left[\tau_a - \tfrac{1}{10}\tau_a,\ \tau_a + \tfrac{1}{10}\tau_a\right]$$

Uncertainty also exists in the parameters ω_n and ζ used to model the rotor mast-flexing mode. The description of this mode is considered quite reliable, but uncertainty in the parameters ω_n and ζ is approximated conservatively at $\pm\frac{1}{5}$ of their nominal values. Therefore, the parameters ω_n and ξ are believed to lie in the bounded region

$$\left[\omega_n - \tfrac{1}{5}\omega_n,\ \omega_n + \tfrac{1}{5}\omega_n\right], \qquad \left[\zeta - \tfrac{1}{5}\zeta,\ \zeta + \tfrac{1}{5}\zeta\right]$$

To allow the low-frequency system/model mismatch dynamics to cover a larger range of frequencies, parametric uncertainty is included in the coefficients used to model these dynamics. The coefficients τ_m and τ_t, which model the low-frequency system/model mismatch, are extended to cover the range of values

$$\left[\tau_m - \tfrac{1}{3}\tau_m,\ \tau_m + \tfrac{1}{3}\tau_m\right], \qquad \left[\tau_t - \tfrac{1}{3}\tau_t,\ \tau_t + \tfrac{1}{3}\tau_t\right]$$

This as also true of the coefficient used to model the high-frequency unmodeled dynamics. Uncertainty increases at high frequencies; thus, the coefficient τ_d is assumed to lie in the larger interval

$$\left[\tau_d - \tfrac{1}{2}\tau_d,\ \tau_d + \tfrac{1}{2}\tau_d\right]$$

III. Handling Qualities Specifications

The handling qualities assessment for a helicopter is a measure of the facility of maneuvering and stabilizing the aircraft as experienced by the pilot. The standard rotorcraft handling qualities specifications are found in ADS-33C (Ref. 25), which quantifies the minimum acceptable parameters defining the aircraft dynamics. The specification is dependent on the task to be performed (such as precision hover) and the environment in which the aircraft is to be flown. Pilot environment cues are ranked on a usable cue environment (UCE) scale, ranging from 1 (normal daylight visual environment) to 3 (extremely poor visual environment). The UCE and the task to be performed are then combined and the specification indicates the type of response for the application. For example, to perform a precision hover in a UCE of 2, an attitude command attitude hold (ACAH) response in pitch and roll, plus rate command heading hold in vertical and yaw, is specified. This implies that in pitch and roll a unit pilot input will command a unit attitude change in the aircraft. A unit pilot input in vertical or yaw results in a unit rate response.

The small amplitude pitch, roll, and yaw bandwidths are to be at least 3 rad/s. So that collective input to yaw output is not objectionable, the maximum magnitude of the ratio of yaw rate experienced divided by the vertical translation rate should be kept to less than 0.15. The vertical rate response will appear roughly as a closed-loop first-order response, with additional high-frequency phase lag due to high-order dynamics. For level one handling qualities, the time constant of this response shall be not less than 0.2 s^{-1}.

IV. Model-Following Optimization

The use of model-following design is natural in situations where the closed-loop performance objectives are expressed in terms of target transfer functions.[2] In the following technique, linear quadratic regulator (LQR) theory is used to minimize the error transients between the responses of the actual plant and those of the target model.

A. Ideal Target Model

According to the handling qualities specification, the desired closed-loop system is to be low in order; thus, the target model is chosen as having low-order dynamics. Moreover, to meet or exceed the handling qualities specification, the model will be selected with zero cross coupling. Finally, the low-order on-axis responses are specified. The pitch attitude enters in a negative sense, as nose-down pitch should induce a positive forward velocity. The yaw and vertical axis responses should follow similar first-order responses, except with inputs as tail rotor collective and collective, respectively; namely,

$$\dot{R} = -\lambda_R R + \lambda_R r_R, \qquad \dot{W} = -\lambda_W W + \lambda_W r_W$$

From physical arguments, the pitch and roll attitude responses must take into account the pitch and roll rates, thus giving second-order responses written as

$$\dot{Q} = -2\zeta_\theta \omega_\theta Q - \omega_\theta^2 \theta - \omega_\theta^2 r_\theta$$

$$\dot{P} = -2\zeta_\phi \omega_\phi P - \omega_\phi^2 \phi + \omega_\phi^2 r_\phi$$

Combining these equations into a state-space model yields the ideal target model

$$\dot{\tilde{\boldsymbol{x}}} = \tilde{A}\tilde{\boldsymbol{x}} + \tilde{B}r \tag{8}$$

where

$$\tilde{A} = \begin{bmatrix} -\lambda_W & 0 & 0 & 0 & 0 & 0 \\ 0 & -2\zeta_\theta\omega_\theta & 0 & 0 & -\omega_\theta^2 & 0 \\ 0 & 0 & -2\zeta_\phi\omega_\phi & 0 & 0 & -\omega_\phi^2 \\ 0 & 0 & 0 & -\lambda_R & 0 & 0 \\ 0 & 1 & 0 & 0 & 0 & 0 \\ 0 & 0 & 1 & 0 & 0 & 0 \end{bmatrix}$$

$$\tilde{B} = \begin{bmatrix} -\lambda_W & 0 & 0 & 0 \\ 0 & -\omega_\theta^2 & 0 & 0 \\ 0 & 0 & \omega_\phi^2 & 0 \\ 0 & 0 & 0 & \lambda_R \\ 0 & 0 & 0 & 0 \\ 0 & 0 & 0 & 0 \end{bmatrix}$$

$$\tilde{\boldsymbol{x}} = \begin{bmatrix} W \\ Q \\ P \\ R \\ \theta \\ \phi \end{bmatrix} = \begin{bmatrix} \text{vertical velocity} \\ \text{pitch rate} \\ \text{roll rate} \\ \text{yaw rate} \\ \text{pitch attitude} \\ \text{roll attitude} \end{bmatrix}$$

$$r = \begin{bmatrix} r_W \\ r_\theta \\ r_\phi \\ r_R \end{bmatrix} = \begin{bmatrix} \text{vertical velocity command} \\ \text{pitch attitude command} \\ \text{roll attitude command} \\ \text{yaw rate command} \end{bmatrix}$$

Angular rates are in units of radians per second, translational rates in meters per second, and attitudes in radians. The units of control input are in terms of pilot stick movement measured in centimeters. Values for the model that meet or exceed specifications are

$$\lambda_U = 4.0, \qquad \lambda_V = 4.0, \qquad \lambda_W = 3.0, \qquad \lambda_R = 5.0$$

$$\omega_\theta = 4.0, \qquad \omega_\phi = 4.0, \qquad \zeta_\theta = 0.7, \qquad \zeta_\phi = 0.7$$

B. Model-Following Optimization

The controller is chosen so that the closed-loop system dynamics attempt to match the ideal target loop dynamics. An H_2 optimization is appropriate that will minimize the error transients between the actual plant and the target model. It is assumed in the model-following optimization that the helicopter is modeled exactly by Eq. (1) and is fully instrumented to provide measurements of all relevant aircraft states where

$$y = C\boldsymbol{x}_h, \qquad C = I_8 \tag{9}$$

Control law design objectives are directly related to the aircraft mission and the corresponding handling qualities specifications. The choice of performance outputs

$$z = Hx_h = \begin{bmatrix} \text{vertical velocity} \\ \text{pitch attitude} \\ \text{roll attitude} \\ \text{yaw rate} \end{bmatrix}$$

$$H = \begin{bmatrix} 0 & 1 & 0 & 0 & 0 & 0 & 0 & 0 \\ 0 & 0 & 0 & 0 & 0 & 0 & 1 & 0 \\ 0 & 0 & 0 & 0 & 0 & 0 & 0 & 1 \\ 0 & 0 & 0 & 0 & 0 & 1 & 0 & 0 \end{bmatrix} \tag{10}$$

is apparent from the response type specified in Sec. III to perform the precision hover task with UCE = 2. To produce the same response in the plant as in the target model, states for feedback and performance outputs of the target model are chosen

$$\tilde{y} = \tilde{C}\tilde{x}, \qquad \tilde{C} = C \tag{11}$$

$$\tilde{z} = \tilde{H}\tilde{x}, \qquad \tilde{H} = H \tag{12}$$

The control will minimize the difference between the model performance (12) and the plant performance (10) by minimizing the model mismatch error

$$\boldsymbol{e}_e = \tilde{\boldsymbol{z}} - \boldsymbol{z} = \tilde{H}\tilde{\boldsymbol{x}} - H\boldsymbol{x}_h \tag{13}$$

Collecting Eqs. (1) and (8), the augmented state may be written as

$$\dot{\boldsymbol{x}}' = A'\boldsymbol{x}' + B'\boldsymbol{u} + G'r, \qquad \boldsymbol{x}' = \begin{bmatrix} \boldsymbol{x}_h \\ \tilde{\boldsymbol{x}} \end{bmatrix}, \qquad A' = \begin{bmatrix} A_h & 0 \\ 0 & \tilde{A} \end{bmatrix}$$

$$B' = \begin{bmatrix} B_h \\ 0 \end{bmatrix}, \qquad G' = \begin{bmatrix} 0 \\ \tilde{B} \end{bmatrix} \tag{14}$$

The tracking problem is modified using the command generator tracker technique[2] so that standard regulator theory may be used. For ACAH systems requiring step input tracking, the reference signal is assumed to satisfy the differential equation

$$\dot{r} = \begin{bmatrix} \dot{r}_W \\ r_\theta \\ r_\phi \\ r_R \end{bmatrix} = \begin{bmatrix} 0 \\ 0 \\ 0 \\ 0 \end{bmatrix} \tag{15}$$

for step commands in each input. Differentiating Eq. (14) and using

$$\boldsymbol{\xi} = \boldsymbol{x}', \qquad \boldsymbol{\theta} = \dot{\boldsymbol{u}} \tag{16}$$

give

$$\dot{\boldsymbol{\xi}} = A'\boldsymbol{\xi} + B'\boldsymbol{\theta} \tag{17}$$

Most important, the reference input (15) does not appear in the modified system (17). Applying the preceding operation to the model mismatch error (13) results in

$$\dot{e}_e = [-H \quad \tilde{H}]\boldsymbol{\xi}, \qquad H' = [-H \quad \tilde{H}] \tag{18}$$

At last, collecting the dynamics of Eqs. (17) and (18) into one system produces

$$\begin{bmatrix} \dot{e}_e \\ \dot{\xi} \end{bmatrix} = \begin{bmatrix} 0 & H' \\ 0 & A' \end{bmatrix} \begin{bmatrix} e_e \\ \xi \end{bmatrix} + \begin{bmatrix} 0 \\ B' \end{bmatrix} \theta \tag{19}$$

so that LQR theory may be used to design a tracking system with model-following behavior. When the augmented state is partitioned as

$$\xi = \begin{bmatrix} \xi_p \\ \xi_m \end{bmatrix}$$

where the subscripts p and m denote plant and model, respectively, and

$$C_e = [I_4 \quad 0_{4\times 16}] \tag{20}$$

is defined, a performance index may be formulated as

$$J = \frac{1}{2}\int_0^\infty \begin{bmatrix} e_e \\ \xi_p \\ \xi_m \end{bmatrix}^T C_e^T Q C_e \begin{bmatrix} e_e \\ \xi_p \\ \xi_m \end{bmatrix} + \theta^T R \theta \, dt \tag{21}$$

The resulting pseudocontrol, which is the derivative of the actual control, is

$$\theta = -K_e e_e - K_p \xi_p - K_m \xi_m \tag{22}$$

Integrating Eq. (22) yields the true control input

$$u = \int \theta \, dt = -K_e \int e_e \, dt - K_p x - K_m \underline{x} \tag{23}$$

Thus, the explicit model-following design results in a dynamic controller because the model appears in the control structure as a feedforward compensator. The model mismatch error (13) is integrated and is also used as part of the feedforward compensation.

V. Mixed-Norm Control

Robust flight control design incorporating H_∞ robust stability and optimal nominal H_2 model-following performance is presented to synthesize a controller designed to improve the handling qualities of the helicopter. It is necessary to piece together the uncertainty description of the linear design model and the model-following optimization into the appropriate mathematical framework for solution.

A. Mathematical Framework

The mixed norm control problem for the helicopter concerns a finite-dimensional linear time-invariant system. A state-space description of the plant G is given by

$$\dot{x} = Ax + B_1 w_1 + B_2 w_2 + B_3 u, \qquad z_1 = C_1 x + D_1 u$$

$$z_2 = C_2 x + D_2 u, \qquad y = x \tag{24}$$

The following standard assumptions are made on G (Refs. 22 and 26):

$$\{A, B_3\} \text{ is stabilizable} \tag{25}$$

$$D_1 \text{ and } D_2 \text{ both have full column rank} \tag{26}$$

For each $\omega \in \Re$ and for $k = 1, 2$

$$\begin{bmatrix} A - j\omega I & B_3 \\ C_k & D_k \end{bmatrix} \tag{27}$$

has full column rank

$$D_2^T [C_2 \quad D_2] = [0 \quad I] \tag{28}$$

Let $T_1(K)$ and $T_2(K)$ denote the closed-loop transfer matrices from w_1 to z_1 and w_2 to z_2, respectively. A given controller K is called admissible (for G) if K is real rational proper, and the minimal realization of K internally stabilizes the state-space realization of G. The mixed norm problem is defined as follows: For the plant G defined in Eq. (24), find an admissible controller K that achieves:

$$\inf \{\|T_1(K)\|_2 : K \text{ admissible and } \|T_2(K)\|_\infty < 1\}$$

There exists an admissible controller K that solves the mixed norm problem if and only if the following conditions hold:

$$H_{2/\infty} \in \text{dom(Ric)}, \qquad X_{2/\infty} := \text{Ric}(H_{2/\infty}) \geq 0 \tag{29}$$

$$J_{2/\infty} \in \text{dom(Ric)}, \qquad Y_{2/\infty} := \text{Ric}(J_{2/\infty}) \tag{30}$$

$$\rho(X_{2/\infty} Y_{2/\infty}) < 1 \tag{31}$$

where $V_2 := \Pi_1 B_2$ and the Hamiltonian matrices are defined as

$$H_{2/\infty} := \begin{bmatrix} A & B_2 B_2^T - B_3 B_3^T \\ -C_2^T C_2 & -A^T \end{bmatrix} \tag{32}$$

$$J_{2/\infty} := \begin{bmatrix} A_F^T & C_{2F}^T C_{2F} \\ -B_2\left(I - V_2^+ V_2\right) B_2^T & -A \end{bmatrix} \tag{33}$$

Under assumption (28), condition (29) is equivalent to the existence of an admissible controller K such that $\|T_2(K)\|_\infty < 1$. Conditions (30) and (31) reflect that one of these admissible controllers must also minimize $\|T_1(K)\|_2$. One more condition is the special case when $\text{im}B_1$ and $\text{im}B_2$ are linearly independent, then conditions (30) and (31) hold and a much stronger result is true.

Consider a feedback system with plant G given by Eq. (24). Suppose that $\text{im}B_2 \cap \text{im}B_1 = 0$. Then the problem is solvable if and only if there exists an admissible controller K such that $\|T_2(K)\|_\infty < 1$. In this case, a solution is given by

$$K := \begin{bmatrix} A_1 & A_1\Omega - \Omega A_{F_1} \\ H - F & F(I - \Omega) + H\Omega \end{bmatrix} \tag{34}$$

where

$$A_1 := A + (I - \Omega)B_3 H + \Omega B_3 F, \qquad A_{F_1} := A + B_3 F$$

$$\Omega := B_2 V_2^+ \Pi_1$$

B. Model Uncertainty Description

The state-space parameter uncertainty of the higher-order model (7) is modeled as variable linear gains in a feedback structure via linear fractional transformations (LFT) represented by a matrix Δ whose parameters are believed to lie in the intervals defined in Sec. II. It is possible to pull out the uncertainties from the system and collect them in Δ via an LFT. Inputs and outputs to Δ are z_2 and w_2, respectively, to follow the controller setup in Eq. (24). As such, the signal w_2 is the output of the model error A, not an exogenous input.[26] The linear design model is then assumed to be described by

$$\dot{x}_{h/e} = A_{h/e/\text{nom}} x_{h/e} + B_{\text{dev}/A} w_2 + B_{h/e} u \tag{35}$$

which is found via the following:

1) Starting with $(A_{h/e}, B_{h/e})$ identify the component in the state transition matrix $A_{h/e}$ associated with the uncertainty specified in Sec. II.

2) Find a range on the uncertain parameter about the nominal midpoint to form a mean state transition matrix $A_{h/e/\text{mean}}$.

3) Construct a B_{dev} in the range space of the uncertain parameter so that $A_{h/e/\text{mean}} + \delta B_{\text{dev}}$ covers the range of all possible uncertainty for the identified component of uncertainty with $|\delta| \leq 1$.

4) Replace the uncertain component in $A_{h/e}$ with its corresponding uncertainty description, $A_{h/e/\text{mean}} + \delta B_{\text{dev}}$.

5) Pull out the δB_{dev} elements to form a matrix $B_{\text{dev}/A}$.

6) $A_{h/e/\text{mean}}$ forms a new nominal component in the state transition matrix.

7) Repeat this for each uncertain component in $A_{h/e}$.

When the algorithm is completed, the state transition matrix $A_{h/e/\text{nom}}$ is created for the system described in Eq. (35), which represents the helicopter dynamics when the uncertain parameters are believed to equal their mean values. The matrix $B_{\text{dev}/A}$ represents the deviation in the matrix $A_{h/e/\text{nom}}$.

C. Model-Following Performance Objective

The model-following objective is accomplished by replacing the lower-order model (1) in Eq. (14) with the higher-order model of the Bell 205 helicopter with mean parameter values, Eq. (35). All other matrices remain the same and are appropriately augmented in size to retain their dimensional compatibility.

D. Mixed H_2/H_∞ Problem Description for the Helicopter

The complete mixed norm problem using Eqs. (19), (21), and (35) is, thus,

$$\begin{bmatrix} \dot{e}_e \\ \dot{\xi}_p \\ \dot{\xi}_m \end{bmatrix} = \begin{bmatrix} 0 & -H & \tilde{H} \\ 0 & A_{h/e/\text{nom}} & 0 \\ 0 & 0 & \tilde{A} \end{bmatrix} \begin{bmatrix} e_e \\ \xi_p \\ \xi_m \end{bmatrix} + B_1 w_1 + \frac{1}{\gamma} \begin{bmatrix} 0 \\ B_{\text{dev}/A} \\ 0 \end{bmatrix} w_2 + \begin{bmatrix} 0 \\ B_{h/e} \\ 0 \end{bmatrix} \theta \tag{36}$$

$$z_1 = \begin{bmatrix} Q^{\frac{1}{2}} C \\ 0 \end{bmatrix} \begin{bmatrix} e \\ \xi_p \\ \xi_m \end{bmatrix} + \begin{bmatrix} 0 \\ R^{\frac{1}{2}} \end{bmatrix} \theta \tag{37}$$

$$z_2 = \gamma \begin{bmatrix} I & 0 & 0 \\ 0 & I & 0 \\ 0 & 0 & I \\ 0 & 0 & 0 \end{bmatrix} \begin{bmatrix} e_e \\ \xi_p \\ \xi_m \end{bmatrix} + \begin{bmatrix} 0 \\ 0 \\ 0 \\ 1 \end{bmatrix} \theta \tag{38}$$

Q and R in Eq. (37) are selected through iteration to achieve desired nominal performance and are selected similar to a standard LQR design. A fictitious uncertainty in the control effort μ is introduced in Eq. (38) to satisfy assumption (28) and scaled by γ to preserve the physical significance of the posed problem. The H_2/H_∞ controller synthesis ignores the known block diagonal structure of the uncertainties, thus, a certain degree of conservativeness to robustness is expected. The matrix B_1 is selected to ensure the range space of B_1 and the range of

$$\begin{bmatrix} 0 \\ B_{\text{dev}/A} \\ 0 \end{bmatrix}$$

are linearly independent.

VI. Results

A. Frequency-Response Results

For desired response to reference command inputs the on-axis frequency response should be 0 dB across the desired bandwidth with off-axis magnitudes no greater than −20 dB for decoupling. Examples of frequency-response plots for the two extreme cases of uncertainty, $\Delta = I_{67}$ and $-0.6 \times I_{67}$, are presented in Figs. 3 and 4 for vertical velocity and roll attitude responses, respectively. The vertical velocity response in Fig. 3 is highly decoupled with a desired closed-loop system bandwidth of 3 rad/s. A resonant peak exists at roughly 14 rad/s in the magnitude plot. This represents the strong influence of the rotor mast-flexing mode and is a good indication that the uncertainty description is correct. The roll attitude command response illustrated in Fig. 4 is also decoupled with a bandwidth frequency at approximately 1.5 rad/s. The pitch and yaw axes show similar responses.

B. Time-Domain Response Results

The envelope of closed-loop system time responses to vertical velocity and roll attitude step command inputs for perturbed plants $\Delta = -0.6 \times I_{67}$, $-0.45 \times I_{67}$, $-0.3 \times I_{67}$, $-0.15 \times I_{67}$, $0.25 \times I_{67}$, $0.5 \times I_{67}$, $0.75 \times I_{67}$, and I_{67} are presented with their corresponding control histories in Figs. 5 and 6, respectively. The desired on-axis response to vertical velocity and yaw rate inputs should be first order, whereas pitch and roll attitude should result in second-order responses. The responses in vertical and yaw should possess a time constant of $\frac{1}{3}$ and $\frac{1}{5}$ s, respectively. Similarly, for the second-order responses in pitch and roll, the time responses should each possess a rise time of 0.45 s and a settling time of 1.5 s, to match the target model. Control effort is bounded by deflection limits of control surface actuators of ±20 cm.

On-axis performance in vertical is sensitive to plant variations with decoupling qualities that are insensitive to plant perturbations. On-axis performance in roll is sensitive to uncertainties in the plant with good decoupling qualities over the uncertainty range. Control is rather insensitive to plant variations with deflections of the actuators well within the accepted limits. Pitch and yaw axes show similar responses.

C. Robust Stability Analysis

The robust stability characteristics of the closed-loop system are evaluated using μ analysis. The fictitious uncertainty in the control μ is removed in Eq. (38) for analysis. The μ plot of the frequency response with real perturbations is illustrated in Fig. 7. The peak

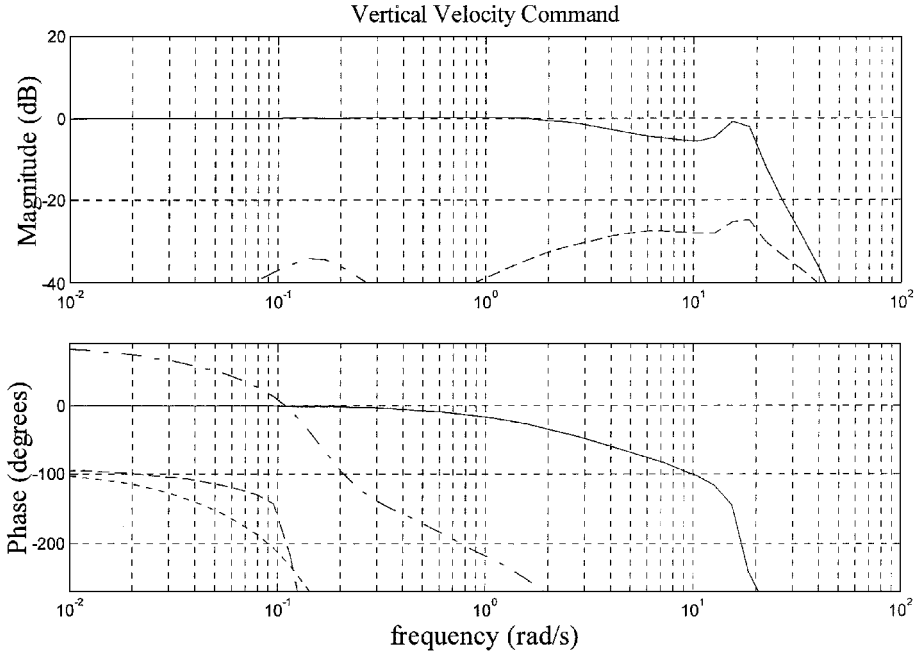

Fig. 3 Frequency response of the closed-loop system to vertical velocity command input for the perturbed plant $\Delta = I_{67}$: ——, vertical velocity; - - -, pitch attitude; – – –, roll attitude; and — —, yaw rate.

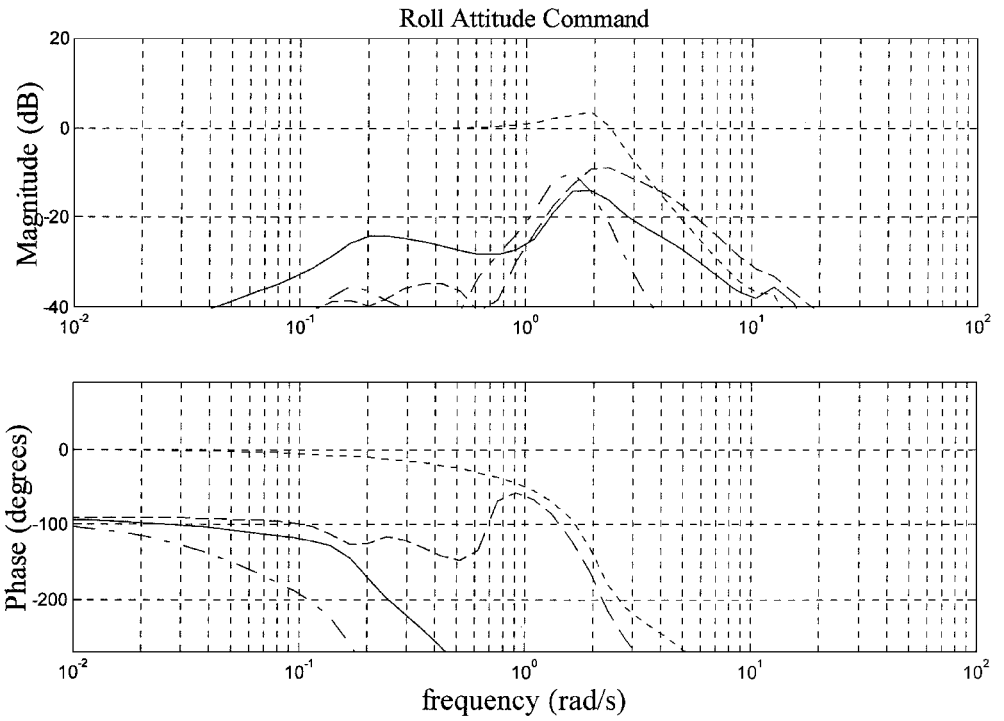

Fig. 4 Frequency response of the closed-loop system to roll attitude command input for the perturbed plant $\Delta = -0.6 \times I_{67}$: ——, vertical velocity; - - -, pitch attitude; - - -, roll attitude; and — —, yaw rate.

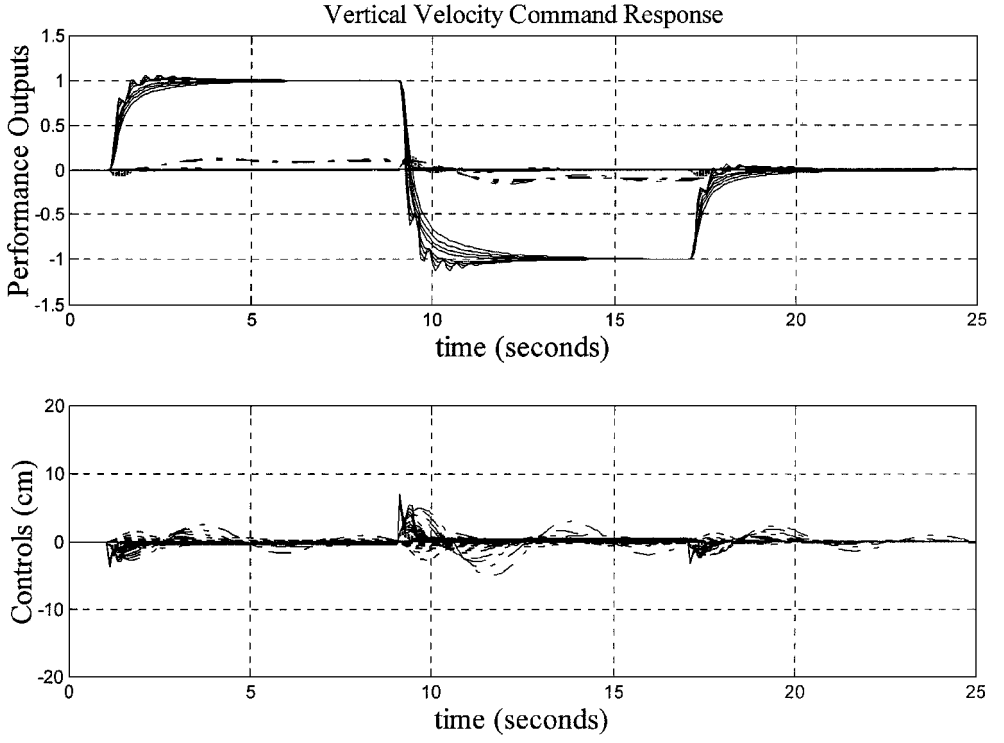

Fig. 5 Envelope of mixed-norm closed-loop system time responses to vertical velocity step input command for perturbed plants $\Delta = -0.6 \times I_{67}$, $-0.45 \times I_{67}$, $-0.3 \times I_{67}$, $-0.15 \times I_{67}$, $0.25 \times I_{67}$, $0.5 \times I_{67}$, and $0.75 \times I_{67}$: ——, vertical velocity; - - -, pitch attitude; - - -, roll attitude; — —, yaw rate; ——, collective; - - -, longitudinal cyclic; - - -, lateral cyclic; and — —, tail.

value of 1.3 for the upper bound of μ implies that there is a diagonal, real perturbation of size $\frac{1}{1.3}$, or approximately 0.77, that causes instability. In other words, the use of μ implies that the range of values covered by the uncertain parameters in Sec. II must be decreased by a factor of 0.77 to ensure stability. The use of μ analysis implies a worst-case analysis, and so it must be weighed with qualitative arguments concerning the likelihood of worst-case perturbations to determine the significance of the results. The value confirms well with simulation results, where the worst-case time simulation occurs in the negative direction of the uncertainty.

D. Comparison with H_2 Solution

For comparison, an LQR controller is synthesized with Q and R unchanged from Sec. V. The LQR solution minimizes the H_2 norm providing desired optimal nominal performance only, without

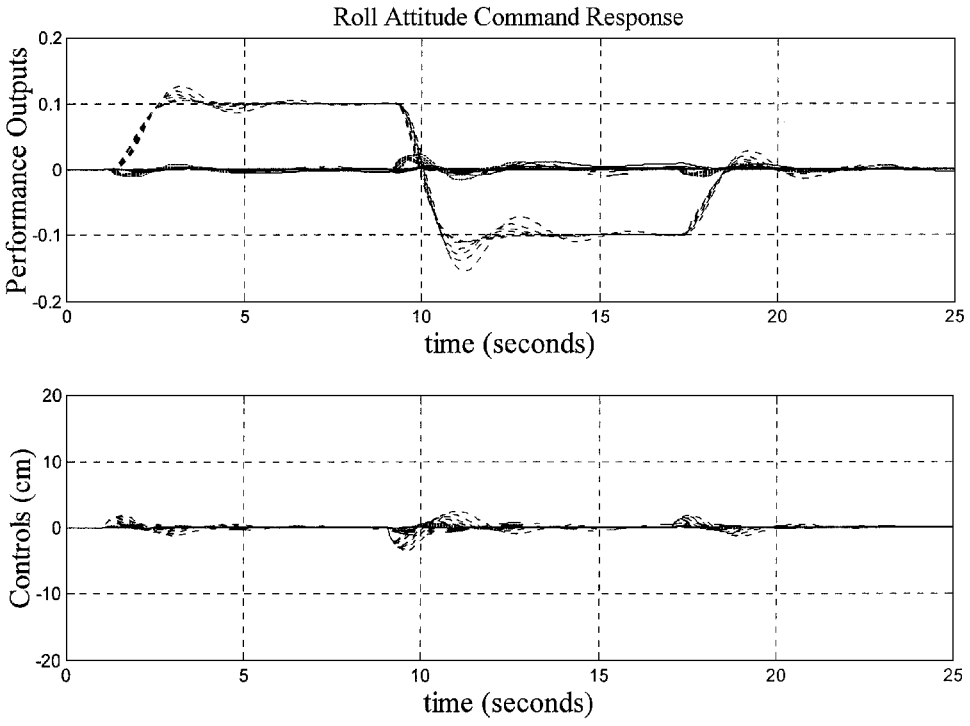

Fig. 6 Envelope of mixed-norm closed-loop system time responses to roll attitude step input command for perturbed plants $\Delta = -0.6 \times I_{67}$, $-0.45 \times I_{67}$, $-0.3 \times I_{67}$, $-0.15 \times I_{67}$, $0.25 \times I_{67}$, $0.5 \times I_{67}$, and $0.75 \times I_{67}$: ——, vertical velocity; - - -, pitch attitude; - - -, roll attitude; ——, yaw rate; ——, collective; - - -, longitudinal cyclic; - - -, lateral cyclic; and ——, tail.

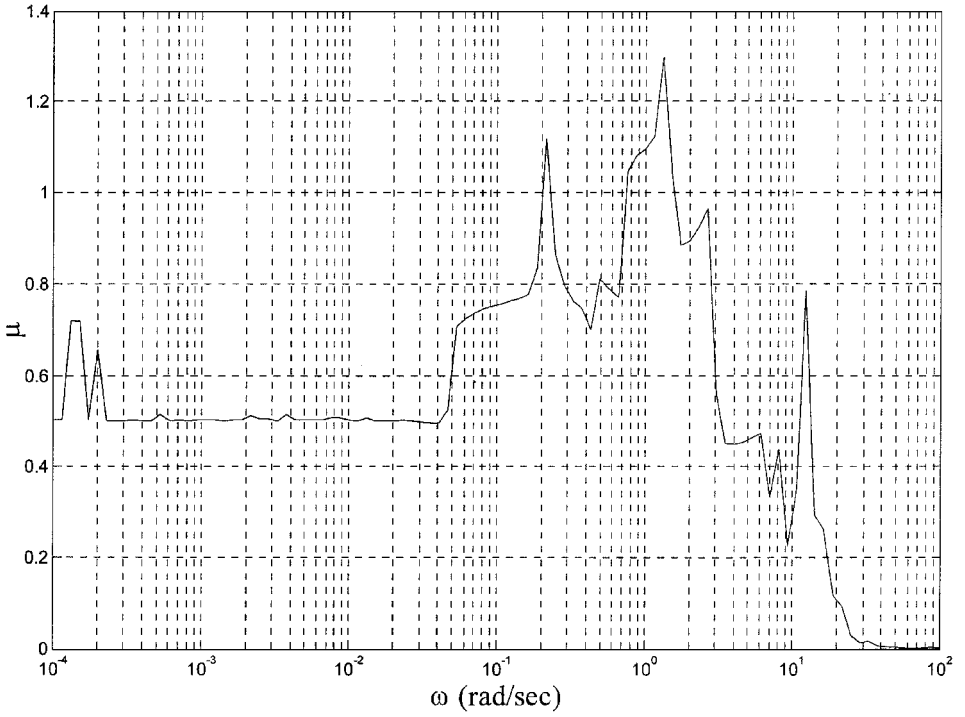

Fig. 7 Plot of θ for robust stability analysis with real uncertainty:——, θ upper bound.

any robustness optimization. A μ analysis is performed on the closed-loop system to determine the robust stability characteristics of the LQR solution. Analysis results in a peak value of the upper bound on $\mu = 1.4$. This is comparable to $\mu = 1.3$ obtained for the closed-loop system with mixed H_2/H_∞-optimal control. The peak values of the upper bounds suggest that the mixed H_2/H_∞ and LQR designs possess similar robust stability characteristics. However, vertical on-axis performance furnished by the LQR controller, depicted in Fig. 8, demonstrates sensitivity to plant variations with poor decoupling qualities and a problematic oscillation in the output. The oscillation occurs at approximately 2.5 Hz, or close to 14 rad/s, the natural frequency of the rotor mast-flexing mode. Thus, LQR control introduces degraded handling qualities and undesirable fatigue concerns to helicopter components. The LQR solution provides optimal nominal performance comparable to that of the mixed H_2/H_∞ design for certain weightings in the cost function. However, in the presence of model variation, the quality of performance provided by the mixed H_2/H_∞ controller is more aptly maintained than that afforded by the LQR controller.

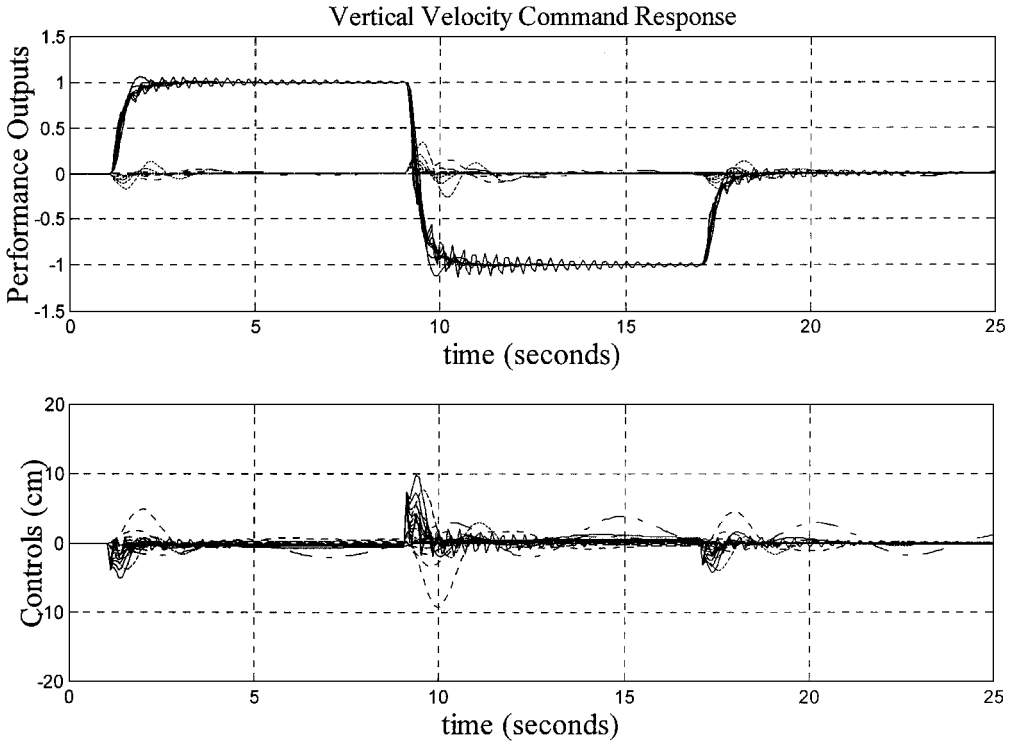

Fig. 8 Envelope of H_2 closed-loop system time responses to vertical velocity step input command for perturbed plants $\Delta = -0.6 \times I_{67}, -0.45 \times I_{67}, -0.3 \times I_{67}, -0.15 \times I_{67}, 0.25 \times I_{67}, 0.5 \times I_{67}$, and $0.75 \times I_{67}$: ——, vertical velocity; - - -, pitch attitude; - - -, roll attitude; — ··—, yaw rate; ——, collective; - - -, longitudinal cyclic; - - -, lateral cyclic; and — ··—, tail.

VII. Summary

This study has shown the efficacy of designing control systems for helicopters in that the multiobjective nature of the system and design are exemplified. On-axis performance is inherently restricted by the goal of not only low cross coupling (as per many modern control designs) but also robustness to model and dynamic uncertainties. The mixed-norm approach considered here handles these conflicting goals in a relatively efficient manner.

Experimental frequency responses of the Bell 205 helicopter provide a clear and reliable picture of the uncertainty in aircraft dynamics between the nominal model and the actual aircraft. These dynamics are quantified and incorporated into a linear design model that more accurately describes the true aircraft to reduce the tradeoff between performance and robustness in design and permit higher achievable performance. The real-world control problem is formulated into a mathematical framework to provide optimal nominal model following performance of a well-defined target model. An LFT of the uncertain system dynamics is used as a natural way of modeling structured uncertainty in the linear design model. This description is formulated to naturally describe stability margins in view of the small gain theorem.

The addition of a robust stability constraint creates a multiobjective control problem, and so a mixed-norm controller is formulated to include genuine system requirements without compromise. Finally, structured singular value analysis of system robustness is used to identify acceptable variation in aircraft dynamics within a well-defined uncertainty structure for which stability is assured. The FCS is found to improve the handling qualities of the aircraft by providing dynamic responses in simulation for the aircraft that closely match stringent U.S. Army handling qualities specifications.

References

[1]Padfield, G. D., *Helicopter Flight Dynamics: The Theory and Application of Flying Qualities and Simulation Modeling*, AIAA Education Series, AIAA, Reston, VA, 1996.

[2]Stevens, B. L., and Lewis, F. L., *Aircraft Control and Simulation*, Wiley, New York, 1992.

[3]Pieper, J. K., Baillie, S., and Goheen, K. R., "Linear-Quadratic Optimal Model-Following Control of a Helicopter in Hover," *Optimal Control Applications and Methods*, Vol. 17, No. 2, 1996, pp. 123–140.

[4]Parry, D. L. K., and Murray-Smith, D. J., "The Application of Model Control Theory to the Single Rotor Helicopter," *Proceedings of the 11th European Rotorcraft Forum*, No. 78, 1985.

[5]Manness, M. A., Gribble, J. J., and Murray-Smith, D. J., "Multivariable Methods for Helicopter Flight Control Law Design," *Proceedings of the 16th European Rotorcraft Forum*, 1990.

[6]Low, E., and Garrard, W., "Design of Flight Control Systems to Meet Rotorcraft Handling Qualities Specifications," *Proceedings of the AIAA Guidance, Navigation, and Control Conference*, AIAA, Washington, DC, 1991, pp. 1381–1391.

[7]Garrard, W. L., and Liebst, B. S., "Design of a Multivariable Flight Control System for Handling Qualities Enhancement," *Journal of the American Helicopter Society*, Vol. 35, No. 4, 1990, pp. 23–30.

[8]Samblancatt, C., Apkarian, P., and Patton, R. J., "Improvement of Helicopter Robustness and Performance Control Law Using Eigenstructure Techniques and H_∞ Synthesis," *16th European Rotorcraft Forum*, 1990.

[9]Manness, M. A., and Murray-Smith, D. J., "Aspects of Multivariable Flight Control Law Design for Helicopters Using Eigenstructure Assignment," *Journal of the American Helicopter Society*, Vol. 18, No. 1, 1992, pp. 18–32.

[10]Postlethwaite, I., and Walker, D. J., "Advanced Control of High Performance Rotorcraft," *Institute of Mathematics and Its Application Conference on Aerospace Vehicle Dynamics and Control*, Cranfield Inst. of Technology, Cranfield, UK, 1992, pp. 615–619.

[11]Pieper, J. K., "Application of SLMC: TRC Control of Helicopter in Hover," *Proceedings of the American Control Conference*, 1995, pp. 1191–1195.

[12]Takahashi, M. D., "Synthesis and Evaluation of an H_2 Control Law for a Hovering Helicopter," *Journal of Guidance, Control, and Dynamics*, Vol. 16, No. 3, 1993, pp. 579–584.

[13]Yue, A., and Postlethwaite, I., "Improvement of Helicopter Handling Qualities Using H_∞ Optimization," *IEE Proceedings Part D Control Theory and Applications*, Vol. 137, 1990, pp. 115–129.

[14]Doyle, J. C., Zhou, K., and Bodenheimer, B., "Optimal Control with Mixed H_2 and H_∞ Performance Objectives," *Proceedings of the American Control Conference*, 1989, pp. 2065–2070.

[15]Bernstein, D. S., and Haddad, W. H., "LQG Control with an H_∞ Performance Bound: A Riccati Equation Approach," *IEEE Transactions on Automatic Control*, Vol. AC-34, No. 3, 1989, pp. 293–305.

[16]Zhou, K., Doyle, J., Glover, K., and Bodenheimer, B., "Mixed H_2 and H_∞ Control," *Proceedings of the American Control Conference*, 1990, pp. 2502–2507.

[17]Yeh, H. H., Banda, S. S., and Chang, B. C., "Necessary and Sufficient Conditions for Mixed H_2 and H_∞ Optimal Control," *Proceedings of the*

29th Conference on Decision and Control, IEEE Publications, Piscataway, NJ, 1988, pp. 1013–1017.

[18]Mustafa, D., and Glover, K., "Controllers Which Satisfy a Closed-Loop H_∞ -Norm Bound and Maximize an Entropy Integral," *Proceedings of the 27th Conference on Decision and Control*, IEEE Publications, Piscataway, NJ, 1989, pp. 959–964.

[19]Mustafa, D., and Glover, K., "Minimum Entropy H_∞ Control," *Lecture Notes in Control and Information Sciences*, Springer-Verlag, New York, 1990.

[20]Khargonekar, P. P., and Rotea, M. A., "Mixed H_2 and H_∞ Control: A Convex Optimization Approach," *IEEE Transactions on Automatic Control*, Vol. AC-36, No. 7, 1991, pp. 824–837.

[21]Hall, S. R., and How, J. P., "Mixed H_2/μ Performance Bounds Using Dissipation Theory," *Proceedings of the IEEE Conference on Decision and Control*, IEEE Publications, Piscataway, NJ, 1993, pp. 1536–1541.

[22]Rotea, M. A., and Khargonekar, P. P., "H_2-Optimal Control with an H_∞ -Constraint: The State Feedback Case," *Automatica*, Vol. 27, No. 8, 1991, pp. 307–316.

[23]Sattler, D. E., "The National Aeronautical Establishment Airborne Simulation Facility," *NAE Misc. 58*, Canadian Aeronautics and Space Inst., Ottawa, 1984.

[24]Heffley, R. K., Jewell, W. F., Lehman, J. M., and Van Winkel, R. A., "A Compilation of Helicopter Handling Qualities Data," CR NAS2-9344, 1979.

[25]Hoh, R. H., Mitchell, D. G., Aponso, B. L., Key, D. L., and Blanken, C. L., "Proposed Specification for Handling Qualities of Military Rotorcraft, Vol. 1—Requirements," U.S. Army Aviation Systems Command, TR 87-A-4, Washington, DC, April 1988.

[26]Green, M., and Limebeer, D. J. N., *Linear Robust Control*, Prentice–Hall, Upper Saddle River, NJ, 1995.